ACCOUNTS
of chemical research

Chemistry and Biology in Femtoliter and Picoliter Volume Droplets

DANIEL T. CHIU* AND ROBERT M. LORENZ
Department of Chemistry, University of Washington, Box 351700, Seattle, Washington 98195-1700

RECEIVED ON OCTOBER 31, 2008

CONSPECTUS

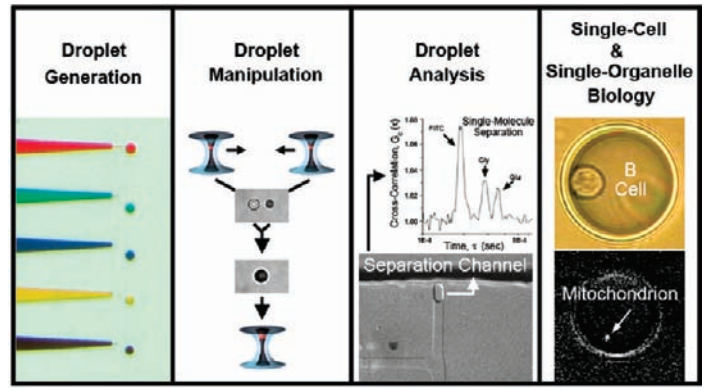

The basic unit of any biological system is the cell, and malfunctions at the single-cell level can result in devastating diseases; in cancer metastasis, for example, a single cell seeds the formation of a distant tumor. Although tiny, a cell is a highly heterogeneous and compartmentalized structure: proteins, lipids, RNA, and small-molecule metabolites constantly traffic among intracellular organelles. Gaining detailed information about the spatiotemporal distribution of these biomolecules is crucial to our understanding of cellular function and dysfunction. To access this information, we need sensitive tools that are capable of extracting comprehensive biochemical information from single cells and subcellular organelles. In this Account, we outline our approach and highlight our progress toward mapping the spatiotemporal organization of information flow in single cells.

Our technique is centered on the use of femtoliter- and picoliter-sized droplets as nanolabs for manipulating single cells and subcellular compartments. We have developed a single-cell nanosurgical technique for isolating select subcellular structures from live cells, a capability that is needed for the high-resolution manipulation and chemical analysis of single cells. Our microfluidic approaches for generating single femtoliter-sized droplets on demand include both pressure and electric field methods; we have also explored a design for the on-demand generation of multiple aqueous droplets to increase throughput.

Droplet formation is only the first step in a sequence that requires manipulation, fusion, transport, and analysis. Optical approaches provide the most convenient and precise control over the formed droplets with our technology platform; we describe aqueous droplet manipulation with optical vortex traps, which enable the remarkable ability to dynamically "tune" the concentration of the contents. Integration of thermoelectric manipulations with these techniques affords further control. The amount of chemical information that can be gleaned from single cells and organelles is critically dependent on the methods available for analyzing droplet contents. We describe three techniques we have developed: (i) droplet encapsulation, rapid cell lysis, and fluorescence-based single-cell assays, (ii) physical sizing of the subcellular organelles and nanoparticles in droplets, and (iii) capillary electrophoresis (CE) analysis of droplet contents.

For biological studies, we are working to integrate the different components of our technology into a robust, automated device; we are also addressing an anticipated need for higher throughput. With progress in these areas, we hope to cement our technique as a new tool for studying single cells and organelles with unprecedented molecular detail.

Introduction

To construct a quantitative model of cellular function, we must obtain new experimental information about the spatiotemporal organization of information flow in these complex systems. Currently, there are two general approaches for conducting measurements on biological systems: microscopy-based methods (e.g., fluorescence microscopy) that offer exquisite spatiotemporal

Published on the Web 03/05/2009 www.pubs.acs.org/acr
10.1021/ar8002464 CCC: $40.75

views of protein trafficking and cellular function but offer little chemical information or bulk biochemical analysis (e.g., mass spectrometry) that provides excellent chemical information but in the process compromises spatiotemporal information. To address this disconnect, we are developing techniques by which we can extract detailed chemical information from subcellular structures and organelles from live cells, while preserving the spatiotemporal information offered by high-resolution microscopy. Our approach is to use single-cell nanosurgery techniques to first isolate subcellular structures of interest and then perform chemistry on the structure in femtoliter-volume aqueous droplets.

Single-Cell Nanosurgery. We are developing and characterizing various optical methods for the selective isolation of subcellular structures and organelles from live cells.[1−5] Briefly, we can remove in real time single fluorescently labeled organelles from a wide-range of cells and have characterized the viability of cells after nanosurgery; we have also identified the critical step in our nanosurgical procedure that causes cell stress.[3]

Besides the viability of the operated cells, it is critical to maintain the integrity of the isolated subcellular structures or organelles. To manipulate and transport the isolated structure, single-beam-optical-gradient trap, or optical tweezers, is a logical choice. Unfortunately, while optical tweezers offers exquisite sensitivity in their ability to position microparticles and to measure the forces exerted by biological motors, they suffer from one important disadvantage: the trapped particle is localized at the laser focus where light intensity is the highest, often reaching 10^7-10^8 W/cm^2.[1,2] As a result, the laser light used to trap a particle also has a propensity to photobleach the particle via multiphoton processes. To minimize this drawback, we have developed a polarization-shaped optical vortex trap for the manipulation of subcellular structures,[1] where the particle is not trapped at the center of the highest laser intensity but is centered at a dark point where minimal laser light is present. Figure 1 shows one example, in which we isolated a single lysosome labeled with Lysotracker (a lysosome-specific dye stain) from within a B lymphocyte.

Chemistry in Small Volumes. To profile and quantify the biochemical contents of subcellular compartments, it is necessary to manipulate chemically (e.g., derivatization reactions) the contents of the nanometer-sized compartments. Here, the main challenge is to overcome dilution by spatially confining the chemical reaction to an ultrasmall volume. To achieve this, one can imagine several different approaches, such as the use of microfluidic chambers[6−8] and biomimetic lipid vesicles.[9,10] We have explored the use of these approaches to

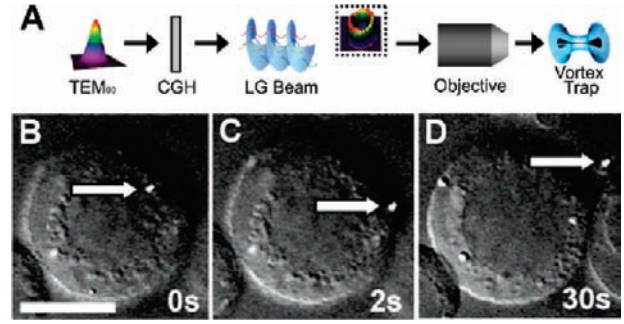

FIGURE 1. (A) Schematic showing the conversion of a Gaussian beam (TEM_{00}) into that of an optical vortex beam (Laguerre−Gaussian (LG) beam) by using a computer generated hologram (CGH) and (B−D) a sequence of images showing the removal of a fluorescent lysosome (stained with Lysotracker Green dye) from a B-lymphocyte. Scale bar = 10 μm in panel B. Reproduced from ref 1. Copyright 2007 American Chemical Society.

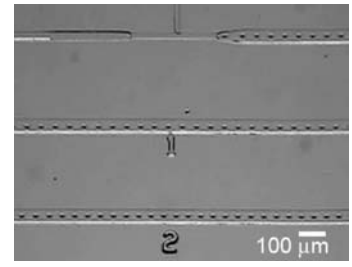

FIGURE 2. Image showing the generation of a steady-state stream of aqueous droplets with a T-junction, a high-throughput technique for droplet creation.

confine chemical reactions, but for our applications, we have determined that aqueous droplets offer the most versatile and robust platform. The rest of this Account will highlight our progress toward using droplets as nanolabs for conducting single-cell and single-organelle experiments.

On-Demand Generation of Single Droplets

The first step in employing droplets as nanoscale reaction vessels is to develop robust techniques for forming droplets of desired sizes, numbers, and compositions. In the past few years, we have witnessed an explosion of activities in the area of droplet microfluidics.[11−18] Here, the two most common microfluidic methods of forming droplets are continuous-stream droplet generation based on a T-channel geometry[11,18] or flow focusing.[19] The continuous-stream method offers high throughput, where thousands of droplets are generated per second. Figure 2 shows an example of continuous-stream droplet generation, where we used a T-channel configuration to form a steady-state stream of droplets.

In contrast to continuous-stream droplet generation, the formation of single droplets on-demand, together with subsequent optical manipulations, offers the possibility to exert precise control over each droplet formed so it can be manip-

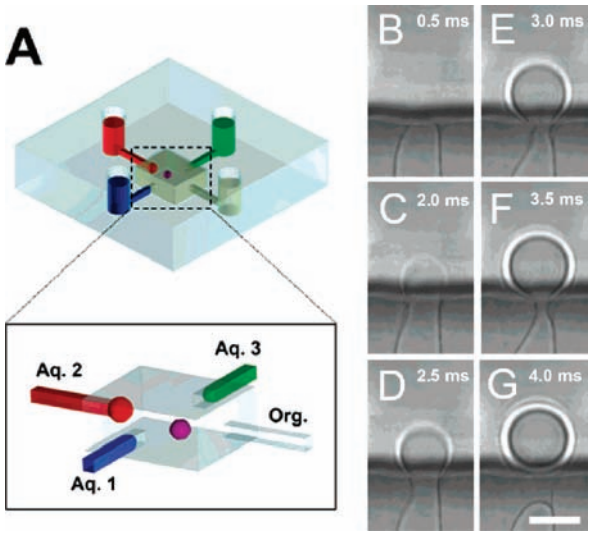

FIGURE 3. (A) Schematic depicting single-droplet generation. The inset shows the inlets with aqueous solutions (aq) of different chemical compositions; org denotes organic oil phase. (B–G) Images showing the generation of a water droplet. The aqueous and immiscible phase initially formed a stable interface at the opening of the inlet channel (B). By slight increase of the pressure of the aqueous phase using a microinjector, a hemidroplet began to grow at the inlet opening (C and D). This growing hemidroplet was connected to the rest of the aqueous phase. To break off the hemidroplet, we quickly withdrew the aqueous phase using the microinjector, which caused a sudden increase in the back-pressure of the aqueous phase. Because the droplet could not respond to this sudden pressure drop in time, necking of the aqueous phase occurred near the opening of the inlet channel (E and F), which led to the final break off of the droplet when the neck was pinched off (G). The scale bar is 4 μm. Reproduced from ref 22. Copyright 2006 American Chemical Society.

ulated and studied with exacting detail.[20–23] Owing to the need to analyze the contents of each droplet with high-information-content techniques, which currently have limited throughput, we have so far been focused on generating single droplets on demand. Here, more elaborate reactions can be conducted, such as multiple and sequential fusions of droplets, and precise droplet positioning for detection. We have developed two techniques for generating single droplets on-demand, one is pressure-based and the other relies on the use of pulsed electric field.

Discrete Pressure-Driven Droplet Generation. Figure 3 shows our chip design,[22] which consists of a main reaction chamber that is surrounded by small inlets. Panels B–G of Figure 3 illustrate the formation of a single droplet. The fine mechanical displacement rendered by the microinjector, together with the high resistance of the inlet channels, offer precise control of the pressure drop across the inlet channels and thus the displacement of the aqueous/oil interface. This attribute permits the facile and controlled formation of individual droplets on-demand.

Discrete Electric-Field-Driven Droplet Generation. This method uses a short (ms) and intense (kV) electric field to deflect the aqueous/oil interface, which leads to the formation of an aqueous jet that breaks off owing to Rayleigh instability.[24,25] Figure 4A shows the schematic of the experimental setup. Figure 4B shows the formation process of a single water droplet with an electric pulse (800 V, 10 ms). The size of the droplet created is related to the amplitude and duration of the applied pulse as well as the connecting channel dimensions.

Simultaneous Generation of Multiple Discrete Droplets. In continuous-stream droplet generation, droplet formation is usually fast, with a single flow-focusing system or T-junction producing many droplets sequentially over a period of time, typically in the range of many hertz to kilohertz. While this approach offers high throughput, there is to some extent a sacrifice of control of the droplets. In discrete droplet generation, exquisite control over individual droplets is afforded with these techniques but at the expense of throughput. To address partially this compromise between control and throughput, we have explored a microfluidic design for the on-demand generation of multiple aqueous droplets with varying chemical contents or concentrations. This method for generating simultaneously multiple aqueous droplets relies on using programmed infusion and withdrawal of immiscible oils into and out of small nozzles where the aqueous solutions reside. Figure 5A shows an image of five droplets being formed simultaneously, and Figure 5B illustrates the use of this system for studying enzymatic activity.[26]

Droplet Manipulations

In using droplets as reaction vessels, their formation is only the first step in a sequence that requires droplet manipulation, fusion, transport, and analysis. Different physical mechanisms might be applied to achieve this, such as the use of dielectrophoresis,[27] magnetic fields,[28] and thermal gradients.[29,30] In fact, we found electrowetting is not limited to moving droplets in contact with a surface[31] but can also be employed to transport droplets dispersed in oil.[32] For a continuous stream of droplets, a number of passive techniques have been developed for droplet sorting, splitting, and fusion.[33,34] With our technology platform and downstream applications, however, we have determined that optical approaches provide the most convenient and precise control over the formed droplets. Below, we will highlight some of our progress in this area.

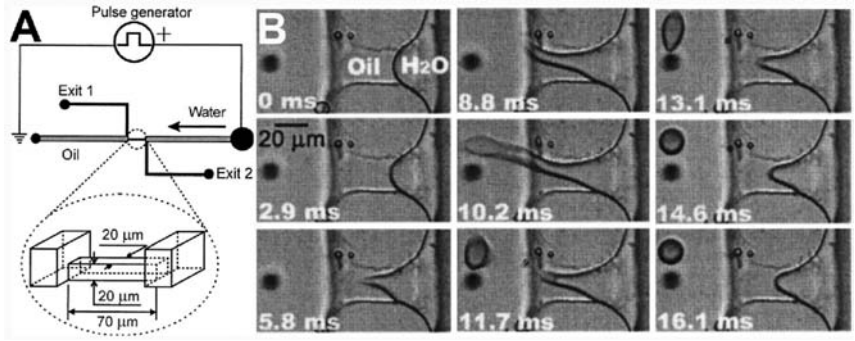

FIGURE 4. (A) Schematic of the experimental setup and (B) sequence of images showing droplet formation initiated by a single voltage pulse (800 V, 10 ms): upon pulse initiation, the interfacial curvature increased, and soon outgrew its symmetrical shape at 5.8 ms. A water jet then protruded into oil rapidly and reached the maximum length at the end of the pulse (10.2 ms), after which the jet broke off and formed the droplet. Reprinted with permission from ref 25. Copyright 2005 American Institute of Physics.

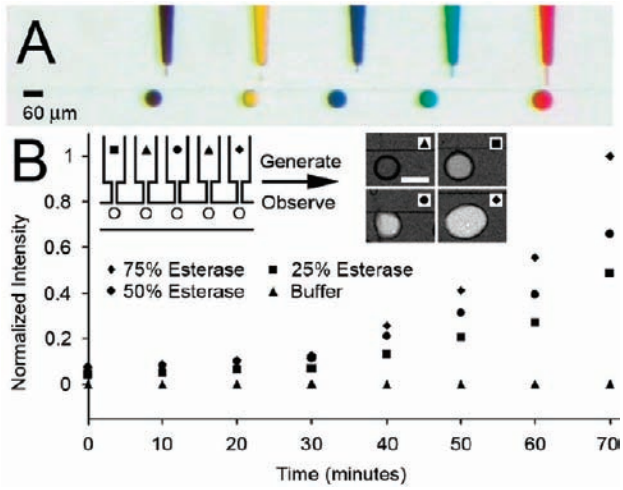

FIGURE 5. (A) Simultaneous generation of multiple droplets containing differing dye solutions and (B) plots of normalized fluorescence intensities as a function of time for droplets containing different concentrations of esterase. The percent esterase refers to the concentration of each esterase solution with respect to the stock solution (0.33 mg mL^{-1} esterase dissolved in phosphate-buffered saline at pH 7.4). The buffer solution contained the same amount of substrate but with no esterase. The inset shows a schematic of the channel layout as well as an image of each type of droplet. The scale bar for the images represents 75 μm. Reprinted from ref 26. Copyright 2008 with permission from Elsevier.

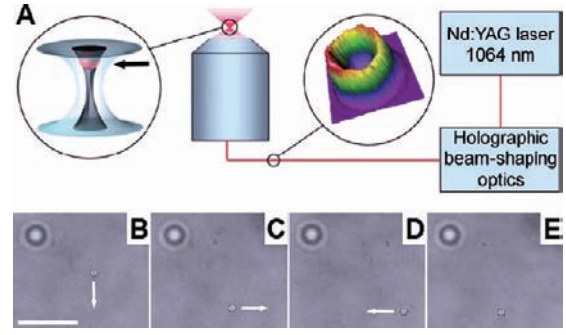

FIGURE 6. (A) The vortex trap was formed by sending a Gaussian laser beam (TEM_{00}) through a microfabricated hologram to form the Laguerre−Gaussian (LG) beam, or optical vortex, after which the desired LG mode was selected and spatially filtered, then used for vortex trapping. The arrow indicates the trapping position of a droplet in the vortex trap. (B−E) Images depicting the trapping and translation of an aqueous droplet (in focus). The arrow denotes the direction of translation of the vortex trap, illustrated using the surface bound droplet in the top left as a reference (out of focus). The scale bar in panel B represents 10 μm. Reprinted with permission from ref 21. Copyright 2007 Wiley-VCH Verlag GmbH & Co. KGaA.

Manipulating Aqueous Droplets with Optical Vortex Traps. To manipulate single aqueous droplets, optical tweezers are an attractive technique because they offer the benefits of being flexible with respect to chip designs and are noninvasive. We found, however, that optical tweezers cannot be applied to the manipulation of aqueous droplets dispersed in an immiscible medium. Optical tweezers trap high refractive index (*n*) particles in a low refractive index medium, such as beads or cells dispersed in an aqueous buffer. Unfortunately, aqueous droplets with an index of refraction of 1.33 are usually of lower refractive index than the surrounding immiscible medium (except for fluorinated oils),[35] in which case optical tweezers will displace rather than trap the droplet. To overcome this issue, we have developed an optical vortex trap. Figure 6A illustrates our scheme for vortex trapping of aqueous droplets, where the ring of laser intensity that surrounds the dark core effectively acts as a light cage for the manipulation of the light-confined droplet (see left inset in Figure 6A).[4,21−23,36]

In the trapping of aqueous droplets, the ring of laser intensity effectively forms a light cage that repels the trapped droplet and thus confines the droplet to the dark core. Similarly, this ring of laser intensity repels and excludes surrounding aqueous droplets and prevents them from entering the vortex trap. The ability of the vortex trap to isolate the trapped droplet is useful, because this prevents uncontrolled droplet

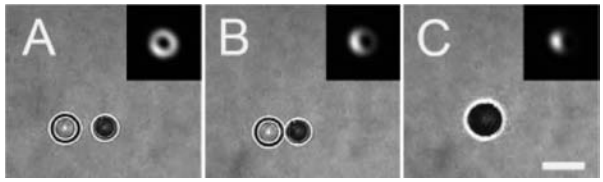

FIGURE 7. Vortex-trap induced fusion of two aqueous droplets. The insets depict changes in the intensity profile of the vortex trap as the hologram was displaced. The scale bar represents 10 μm. Reproduced from ref 23. Copyright 2007 American Chemical Society.

interactions and fusion and preserves the chemical content of the trapped droplet. Unfortunately, this same feature also impairs its ability to induce droplet fusion. We discovered, however, that a lateral displacement of the hologram in a direction orthogonal to the beam-propagation axis can effect an asymmetric distribution of light intensity within the beam profile, while retaining the phase singularity (dark core) in the +-first-order diffracted field.[23] The practical consequence is that the droplet will track the displacement of the dark core within the beam. By creating two vortex traps with opposite handedness, we can enact the movement and fusion of the aqueous droplets (see Figure 7).[23]

Dynamic Modulation of Chemical Concentration in Aqueous Droplets. One remarkable characteristic of vortex trapping of aqueous droplets, we found, is the ability to tune dynamically the concentration of contained molecules.[21,36,37] Figure 8 shows our experimental findings, in which the optical vortex trap slowly "peeled off" layers of water molecules at the interface of the aqueous and immiscible fluids, thus concentrating the encapsulated molecules that were retained within the droplet. The dominant mechanism that underlies this droplet shrinkage is the localized heating ($\leq$1 K) of the interface where the droplet and vortex beam overlap, which results in a localized solubility increase for water in the organic phase that immediately surrounds the trapped droplet. When the power of the vortex trap is decreased or turned off, the water dissolved in the surrounding oil phase returns to the droplet, thus leading to droplet expansion. We found it is also possible to expand the volume of one droplet (target droplet) beyond its original size by accumulating the water released during the shrinkage of an adjacent droplet (donor droplet). Using a vortex trap, we were able to concentrate species by over 4 orders of magnitude without effecting any noticeable temperature changes ($\leq$1 K) in the system. Dynamic control over the concentrations of dissolved species in a nanoscale reaction vessel provides a new degree of control that was previously difficult to achieve in a macroscopic chemical system.

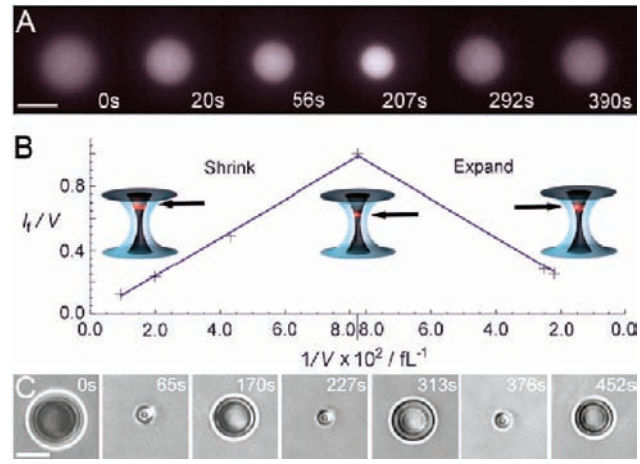

FIGURE 8. (A) Fluorescence images of an aqueous droplet containing ~100 μM dye (Alexa 488) as the droplet went through one cycle of shrinkage and expansion. The scale bar represents 3 μm. (B) Plot of normalized fluorescent intensity per unit volume versus the respective reciprocal volume, depicting species conservation; the insets illustrate the change in the trapping position of the droplet (arrow) in the axial direction as the droplet changes in volume. (C) Images showing three consecutive cycles of droplet shrinkage and expansion, which demonstrates the reversibility of the effect. The scale bar represents 5 μm. Reprinted with permission from ref 21. Copyright 2007 Wiley-VCH Verlag GmbH & Co. KGaA.

Thermoelectric Manipulations of Single Cells in Droplets. Besides the various optical manipulations of droplets, we have recently frozen (and heated) single cells encapsulated in aqueous droplets using thermoelectric coolers.[38] By taking advantage of the vastly different freezing points for aqueous solutions and immiscible oils, we froze a stream of aqueous droplets that were formed on-chip (see Figure 9). By integrating this technique with cell encapsulation into aqueous droplets, we were also able to freeze single cells encased in flowing droplets and determined that the viability of cells was not adversely affected by the process of freezing in aqueous droplets provided cryoprotectants were utilized. When combined with the droplet methodologies described above, this technology has the potential to both selectively heat and cool portions of a chip for a variety of droplet-related applications, such as temperature cycling for cell lysis and PCR or for controlling reaction kinetics.

Analysis of Droplets

In addition to droplet generation and manipulation, the amount of chemical information that can be gleaned from single cells and organelles is critically dependent on the methods that are available for analyzing the contents of droplets. Below, we will describe three techniques that we have devel-

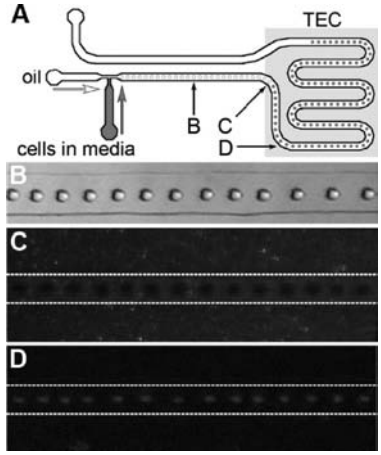

FIGURE 9. (A) Schematic showing the channel system we used for droplet generation (at T-channel) and freezing (above where a thermo-electric cooler (TEC) was placed). (B) Bright-field image of a stream of unfrozen droplets. (C, D) Image of a stream of droplets over the TEC before (C) and after (D) freezing, where the amorphous ice scattered the illumination light and thus appeared "white". Labels in panel A show the positions along the channel where the images shown in panels B–D were taken. Reproduced from ref 38. Copyright 2007 American Chemical Society.

oped so far to readout the contents of femtoliter and picoliter volume droplets.

Droplet Encapsulation, Rapid Cell Lysis, and Fluorescence-Based Single-Cell Assays. The first method is simply based on fluorescence microscopy, owing to the ease of use and sensitivity that fluorescence microscopy provides. Here, we first encapsulate a desired cell or organelle into a droplet, after which we photolyze the cell rapidly and conduct fluorescence-based assays to readout a particular parameter or a very small set of parameters of interest. Figure 10 shows this process in which a single optically trapped B lymphocyte was selectively encapsulated in an aqueous droplet[39] (panels A–D). Once encapsulated within the droplet, the cell was rapidly photolyzed (Figure 10E–H). The attractive aspect of laser photolysis is the rapidity by which the cell can be lysed, so rapid that the cell does not have time to respond and activate its stress signaling pathways.[40] This rapid photolysis, therefore, essentially "freezes" the cellular state at the moment of photolysis and offers a snapshot of the cell's activity at a particular moment in time.

As a demonstration, we used individual droplets as picoliter-sized bioreactors to assay the enzymatic activity of a single cell after single-pulse laser photolysis (panels I–L).[39] Here the droplet confined the lysate and the fluorescent product (fluorescein) within a small finite volume. Without this confinement, both the enzyme and fluorescein would diffuse outward and would be rapidly diluted. Besides the manipulation of single cells, we have also employed this method to

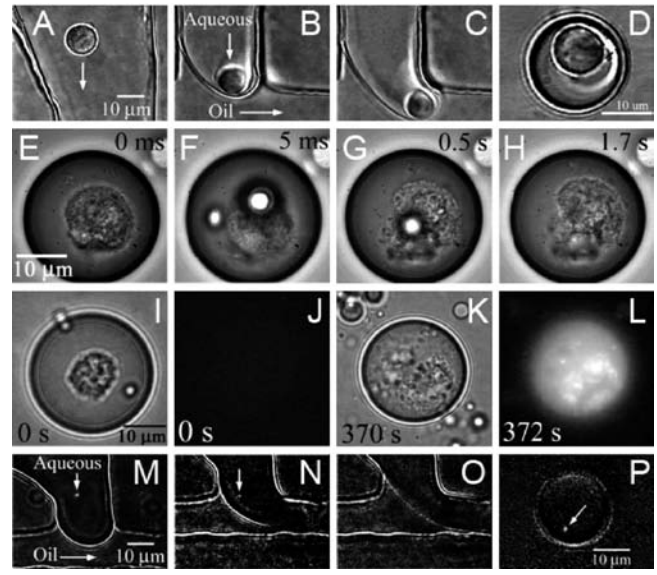

FIGURE 10. (A–C) Optical trapping was used to position the cell close to the water/oil interface; an entrapped cell in a droplet is shown in panel D. (E–H) A video sequence that shows the rapid photolysis of a single cell confined within an aqueous droplet; the pulse energy that we applied was sufficient to form plasma and cavitation bubbles, which rapidly lysed the cell (F, G). (I–L) Single-cell enzymatic assay within an aqueous droplet. (I) A mast cell was encapsulated in an aqueous droplet that contained the fluorogenic substrate fluorescein di-β-D-galactopyranoside (FDG). (J) Prior to photolysis of the cell, there was little fluorescent product within the droplet because the intracellular enzyme β-galactosidase was physically separated from FDG by the cell membrane. (K, L) After laser-induced cell lysis (K), β-galactosidase catalyzed the formation of the product fluorescein, which caused the droplet to become highly fluorescent (L). (M–P) Sequence of images showing the droplet encapsulation of a single mitochondrion. We visualized under fluorescence and optically manipulated a single mitochondrion stained with Mitotracker Green FM at the interface of the two fluids (M, N). Upon application of a pressure pulse to the microchannels (N, O), the mitochondrion was carried away by the flow as the droplet was sheared off (P). Reproduced from ref 39. Copyright 2005 American Chemical Society.

encapsulate single organelles, such as single mitochondria. With this capability, we are currently carrying out various single-organelle assays to understand their heterogeneity, molecular composition, and biological function.

Sizing Subcellular Organelles and Nanoparticles in Droplets. To determine the local concentrations of molecules present within parts of a cell or in a subcellular organelle, it is often necessary to know the size and volume of the organelle. Currently, there are no easy techniques capable of sizing single subdiffraction-limited subcellular particles in free solution. Scanning probe microscopies and electron microscopies require immobilization of the particle on a surface or in a matrix, which makes subsequent solution-phase analysis or transport difficult to perform. Light scattering measurements

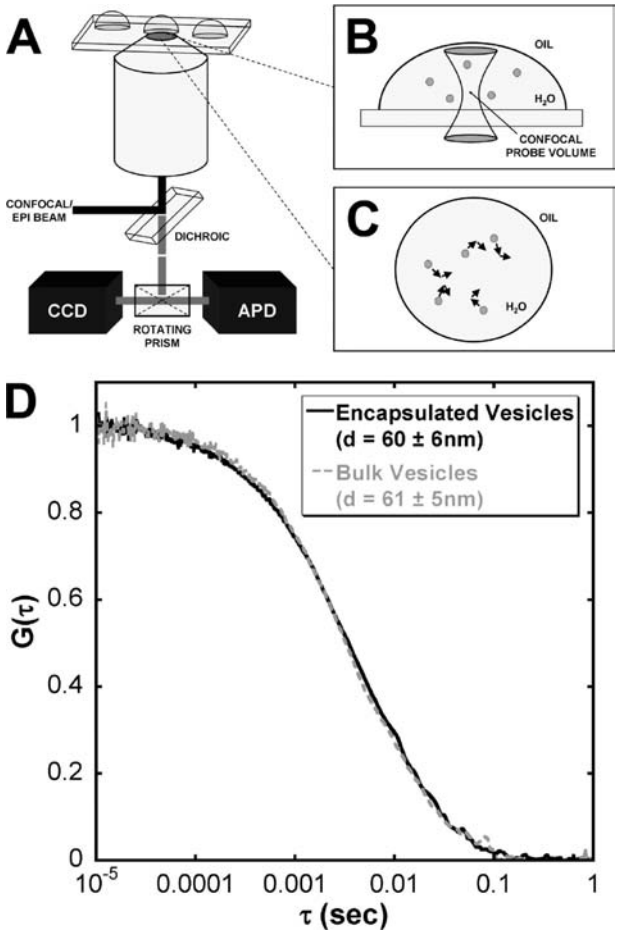

FIGURE 11. In addition to conducting chemical reactions in droplets, size information of encapsulated species can be acquired with correlation spectroscopy. (A–C) Schematic of the setup used to size single molecules or particles encapsulated within droplets, in which correlation spectroscopy used point detection (B) and single-particle tracking employed imaging (C). CCD = camera; APD = avalanche photodiode. (D) Normalized autocorrelation curves of synaptic vesicles encapsulated within a droplet (solid dark gray) and in the bulk solution (dashed light gray), demonstrating that the droplet environment did not affect the measurement. Reproduced from ref 43. Copyright 2008 American Chemical Society.

can size particles in solution but lack sufficient sensitivity to size a single or a small group of particles. To address this need, we have used single aqueous droplets to spatially confine a single or a small group of nanoparticles so their diffusion coefficient and size can be measured using correlation spectroscopy.[41−43] Droplet confinement eliminates the issue of the particle diffusing away from the interrogation region before its diffusion coefficient can be accurately determined. Figure 11 illustrates our experimental design (A–C), in which correlation spectroscopy (B) or single-particle tracking (C) is used to size molecules or nanoparticles in individual droplets; panel D shows the experimental result obtained in sizing synaptic vesicles.

Capillary Electrophoresis (CE) Analysis of Droplet Contents. Despite the numerous methods developed and employed in the past few years for generating and manipulating droplets in microfluidic systems, there is a general lack of strategies for analyzing the contents of droplets, especially small droplets that are in the femtoliter to picoliter range.[20,44,45] Most methods for reading out the contents of droplets rely on fluorescence microscopic imaging, such as our first method described above. These approaches are usually limited to monitoring several species (e.g., with different color dyes) within the droplet and cannot be applied to droplets containing complex mixtures. This limitation is particularly problematic for applications that involve biological studies, owing to the molecular complexity of a cell or organelle. To address this shortcoming, we have developed a CE technique to separate the contents of individual droplets after the contents have been emptied into a separation channel.[20,44] Our approach relies on the use of an immiscible-fluid partition to divide the portion of the fluidic system where droplet generation and manipulation occurs from the part where CE separation takes place; the droplet contents are emptied into the CE channel by fusing the droplet with the immiscible boundary. Figure 12A–F shows the generation of a single droplet, followed by its transport to and fusion with the immiscible partition, thereby emptying the contents of the droplet into the CE channel; subsequent application of an electric field caused CE separation of the droplet contents (panel G, Figure 12).

For many studies that involve single cells, and especially single organelles, the copy number of proteins or other molecules present will likely be very small. As a result, traditional laser-induced-fluorescence detection may lack the necessary sensitivity to detect this small number of molecules after CE separation. For such demanding applications, we must be able to count and identify every analyte molecule present. To achieve this, we have developed a two beam line confocal detection geometry for measuring the electrophoretic mobility of individual molecules undergoing continuous-flow CE separation.[46] This capability is required to analyze the potentially minute amount of analytes present in an aqueous droplet. Figure 13A depicts our experimental design and instrument. To determine the migration time of each molecule that transits between the two spatially offset line-confocal detection regions (panel B), we used two-beam fluorescent cross-correlation spectroscopy (panel C). By maximizing signal-to-background ratio and spatial detection efficiency with line-confocal detection, we have demonstrated an overall

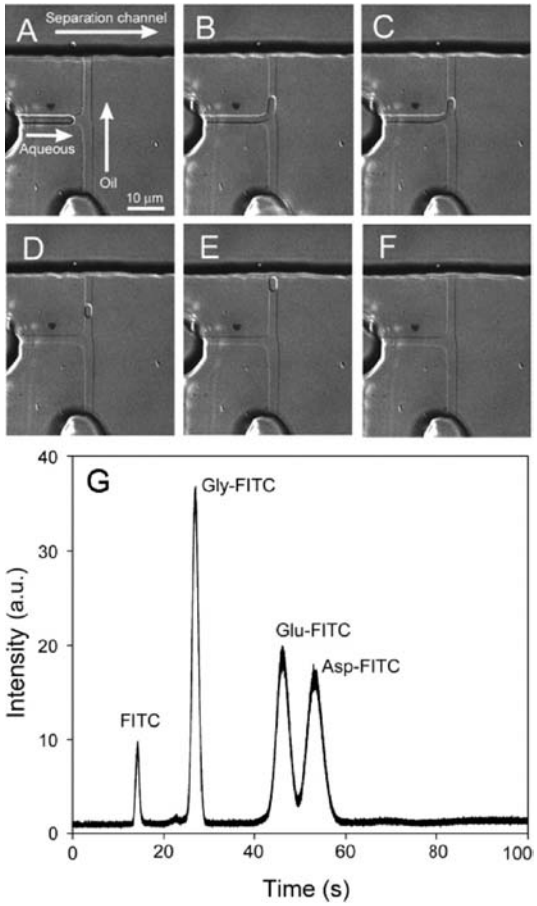

FIGURE 12. Coupling capillary electrophoresis (CE) with droplet microfluidics expands the range of potential applications. (A−F) Images showing the generation and transport of a single aqueous droplet to the CE separation channel. (G) Separation of fluorescein isothiocyanate (FITC)-labeled amino acid (glycine (Gly), glutamic acid (Glu), and aspartic acid (Asp)) contents of a single 10 fL volume droplet; the applied voltage was 500 V/cm, and the separation distance was 2 cm. Reproduced from ref 20. Copyright 2006 American Chemical Society.

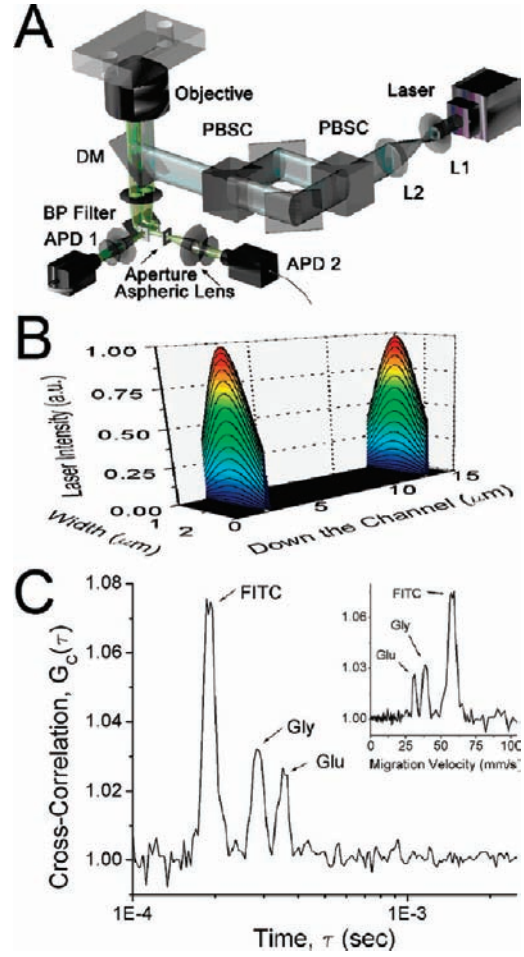

FIGURE 13. (A) Schematic illustrating the setup for continuous-flow single-molecule CE in a micrometer-sized channel: L1,L2 = lens; PBSC = polarizing beam-splitting cube; DM = dichroic mirror; BP = band-pass filter; APD = avalanche photodiode. (B) Simulation showing the distribution of laser intensity across the width of a 2 μm channel for two spatially separated line-confocal detection volumes. (C) Single-molecule continuous-flow CE separation of a mixture of FITC, FITC-labeled glycine, and FITC-labeled glutamate. The inset shows the same data as a function of migration velocity. Reprinted with permission from ref 46. Copyright 2007 Wiley-VCH Verlag GmbH & Co. KGaA.

detection efficiency of greater than 94% for single dye molecules flowing in a 2 μm wide channel. To our knowledge, currently this represents the highest detection efficiency achieved so far for single-molecule CE confined to micrometer-sized channels. It should be noted that even higher detection efficiency can be achieved by confining molecules to nanochannels.[47] Such nanochannels, however, can be difficult to fabricate and work with. Continuous-flow single-molecule CE with nearly complete detection efficiency should prove a versatile tool in the quantification and analysis of samples where the absolute number of molecules is of interest. Further integration with in-droplet single-particle sizing, as described above, will allow us to determine the local concentrations of molecules present within individual compartments of a single cell.

Outlook

This Account highlights some of our recent progress toward using femtoliter and picoliter droplets as nanolabs for single-cell and single-organelle studies. Thus far, our focus has been on developing techniques for generating such small nanoreactors on-demand and on methods to manipulate these reaction vessels with high precision and control. We have also devoted effort to develop sensitive techniques for analyzing the potentially complex contents contained within such small volumes.

To transition our technique toward biological studies, there are two areas that we must address. The first area lies in the integration of the different components of our technology and the

automation of our final device. Integration and automation is needed to ensure our technique is easy to use and robust in operation. The second area that requires additional effort is throughput. We have so far focused on control and precision, but high throughput is often needed for processing thousands of individual samples at a time. For some sample-limited studies, such as circulating cancer cells and stem cells, throughput may not be of the highest priority simply because there are only a few cells available for analysis. For many other experiments, however, throughput is paramount such that an accurate statistical framework can be developed from the analysis of individual organelles and cells. We believe the approach we described here can be adapted for high-throughput operation, because optical techniques can be highly parallelized, such as with holographic methods, and droplet microfluidics can be operated at high speed where droplets are formed at kilohertz rates.

We have started to apply our technique toward several lines of biological studies, such as in understanding the heterogeneities of single mitochondria and individual cancer cells. With further improvements in the two technological areas described above, we hope to cement our technique as a new tool for studying single cells and organelles with unprecedented molecular detail.

This work is supported in part by the National Institutes of Health (Grants EB005197 and GM65293), the National Science Foundation (Grant 0135109), the Keck Foundation, and the Sloan Foundation.

BIOGRAPHICAL INFORMATION

Daniel T. Chiu is currently Professor of Chemistry at the University of Washington, Seattle. He obtained a B.A. in Neurobiology and a B.S. in Chemistry from the University of California at Berkeley in 1993, then a Ph.D. in Chemistry from Stanford University in 1998. After completing postdoctoral research at Harvard University, he started in the Fall of 2000 as an Assistant Professor of Chemistry at the University of Washington. He is currently a member of the Center for Nanotechnology and the Neurobiology and Behavior Program at the University of Washington as well as a member of the Fred Hutchinson Cancer Research Center's Cancer Consortium. His current research is focused on developing new methods for probing complex biological processes at the single-cell and single-molecule level and on applying these new techniques for addressing pressing biological problems.

Robert M. Lorenz received a B.S. degree in Chemistry from the University of North Carolina at Chapel Hill in 2000 and his M.S. and Ph.D. degrees from the University of Washington in 2004 and 2008, respectively. His research focuses on the development of optical and microfluidic techniques for droplet-based single-cell and -organelle studies.

FOOTNOTES

*To whom correspondence should be addressed. E-mail: chiu@chem.washington.edu.

REFERENCES

1 Jeffries, G. D. M.; Edgar, J. S.; Zhao, Y. Q.; Shelby, J. P.; Fong, C.; Chiu, D. T. Using polarization-shaped optical vortex traps for single-cell nanosurgery. *Nano Lett.* **2007**, *7*, 415–420.

2 Kuyper, C. L.; Chiu, D. T. Optical trapping: A versatile technique for biomanipulation. *Appl. Spectrosc.* **2002**, *56*, 300a–312a.

3 Shelby, J. P.; Edgar, J. S.; Chiu, D. T. Monitoring cell survival after extraction of a single subcellular organelle using optical trapping and pulsed-nitrogen laser ablation. *Photochem. Photobiol.* **2005**, *81*, 994–1001.

4 Zhao, Y. Q.; Edgar, J. S.; Jeffries, G. D. M.; McGloin, D.; Chiu, D. T. Spin-to-orbital angular momentum conversion in a strongly focused optical beam. *Phys. Rev. Lett.* **2007**, *99*, 073901.

5 Zhao, Y. Q.; Milne, G.; Edgar, J. S.; Jeffries, G. D. M.; McGloin, D.; Chiu, D. T. Quantitative force mapping of an optical vortex trap. *Appl. Phys. Lett.* **2008**, *92*, 161111.

6 Huang, B.; Wu, H. K.; Bhaya, D.; Grossman, A.; Granier, S.; Kobilka, B. K.; Zare, R. N. Counting low-copy number proteins in a single cell. *Science* **2007**, *315*, 81–84.

7 Marcy, Y.; Ouverney, C.; Bik, E. M.; Losekann, T.; Ivanova, N.; Martin, H. G.; Szeto, E.; Platt, D.; Hugenholtz, P.; Relman, D. A.; Quake, S. R. Dissecting biological "dark matter" with single-cell genetic analysis of rare and uncultivated TM7 microbes from the human mouth. *Proc. Nat. Acad. Sci. U.S.A.* **2007**, *104*, 11889–11894.

8 Rondelez, Y.; Tresset, G.; Tabata, K. V.; Arata, H.; Fujita, H.; Takeuchi, S.; Noji, H. Microfabricated arrays of femtoliter chambers allow single molecule enzymology. *Nat. Biotechnol.* **2005**, *23*, 361–365.

9 Chiu, D. T.; Wilson, C. F.; Ryttsen, F.; Stromberg, A.; Farre, C.; Karlsson, A.; Nordholm, S.; Gaggar, A.; Modi, B. P.; Moscho, A.; Garza-Lopez, R. A.; Orwar, O.; Zare, R. N. Chemical transformations in individual ultrasmall biomimetic containers. *Science* **1999**, *283*, 1892–1895.

10 Karlsson, R.; Karlsson, A.; Ewing, A.; Dommersnes, P.; Joanny, J. F.; Jesorka, A.; Orwar, O. Chemical analysis in nanoscale surfactant networks. *Anal. Chem.* **2006**, *78*, 5960–5968.

11 Song, H.; Chen, D. L.; Ismagilov, R. F. Reactions in droplets in microflulidic channels. *Angew. Chem., Int. Ed.* **2006**, *45*, 7336–7356.

12 Christopher, G. F.; Anna, S. L. Microfluidic methods for generating continuous droplet streams. *J. Phys. D: Appl. Phys.* **2007**, *40*, R319—R336.

13 Huebner, A.; Sharma, S.; Srisa-Art, M.; Hollfelder, F.; Edel, J. B.; Demello, A. J. Microdroplets: A sea of applications. *Lab Chip* **2008**, *8*, 1244–1254.

14 Teh, S. Y.; Lin, R.; Hung, L. H.; Lee, A. P. Droplet microfluidics. *Lab Chip* **2008**, *8*, 198–220.

15 Shui, L.; Eijkel, J. C. T.; van den Berg, A. Multiphase flow in microfluidic systems - Control and applications of droplets and interfaces. *Adv. Colloid Interface Sci.* **2007**, *133*, 35–49.

16 Utada, A. S.; Lorenceau, E.; Link, D. R.; Kaplan, P. D.; Stone, H. A.; Weitz, D. A. Monodisperse double emulsions generated from a microcapillary device. *Science* **2005**, *308*, 537–541.

17 Fuerstman, M. J.; Garstecki, P.; Whitesides, G. M. Coding/decoding and reversibility of droplet trains in microfluidic networks. *Science* **2007**, *315*, 828–832.

18 Thorsen, T.; Roberts, R. W.; Arnold, F. H.; Quake, S. R. Dynamic pattern formation in a vesicle-generating microfluidic device. *Phys. Rev. Lett.* **2001**, *86*, 4163–4166.

19 Anna, S. L.; Bontoux, N.; Stone, H. A. Formation of dispersions using "flow focusing" in microchannels. *Appl. Phys. Lett.* **2003**, *82*, 364–366.

20 Edgar, J. S.; Pabbati, C. P.; Lorenz, R. M.; He, M. Y.; Fiorini, G. S.; Chiu, D. T. Capillary electrophoresis separation in the presence of an immiscible boundary for droplet analysis. *Anal. Chem.* **2006**, *78*, 6948–6954.

21 Jeffries, G. D. M.; Kuo, J. S.; Chiu, D. T. Dynamic modulation of chemical concentration in an aqueous droplet. *Angew. Chem., Int. Ed.* **2007**, *46*, 1326–1328.

22 Lorenz, R. M.; Edgar, J. S.; Jeffries, G. D. M.; Chiu, D. T. Microfluidic and optical systems for the on-demand generation and manipulation of single femtoliter-volume aqueous droplets. *Anal. Chem.* **2006**, *78*, 6433–6439.

23 Lorenz, R. M.; Edgar, J. S.; Jeffries, G. D. M.; Zhao, Y. Q.; McGloin, D.; Chiu, D. T. Vortex-trap-induced fusion of femtoliter-volume aqueous droplets. *Anal. Chem.* **2007**, *79*, 224–228.

24 He, M.; Kuo, J. S.; Chiu, D. T. Effects of ultrasmall orifices on the electrogeneration of femtoliter-volume aqueous droplets. *Langmuir* **2006**, *22*, 6408–6413.

25 He, M. Y.; Kuo, J. S.; Chiu, D. T. Electro-generation of single femtoliter- and picoliter-volume aqueous droplets in microfluidic systems. *Appl. Phys. Lett.* **2005**, *87*, 031916.

26 Lorenz, R. M.; Fiorini, G. S.; Jeffries, G. D. M.; Lim, D. S. W.; He, M. Y.; Chiu, D. T. Simultaneous generation of multiple aqueous droplets in a microfluidic device. *Anal. Chim. Acta* **2008**, *630*, 124–130.

27 Hunt, T. P.; Issadore, D.; Westervelt, R. M. Integrated circuit/microfluidic chip to programmably trap and move cells and droplets with dielectrophoresis. *Lab Chip* **2008**, *8*, 81–87.

28 Nguyen, N. T.; Ng, K. M.; Huang, X. Y. Manipulation of ferrofluid droplets using planar coils. *Appl. Phys. Lett.* **2006**, *89*, 052509.

29 Kotz, K. T.; Noble, K. A.; Faris, G. W. Optical microfluidics. *Appl. Phys. Lett.* **2004**, *85*, 2658–2660.

30 Cordero, M. L.; Burnham, D. R.; Baroud, C. N.; McGloin, D. Thermocapillary manipulation of droplets using holographic beam shaping: Microfluidic pin ball. *Appl. Phys. Lett.* **2008**, *93*, 034107.

31 Fair, R. B. Digital microfluidics: Is a true lab-on-a-chip possible? *Microfluid. Nanofluid.* **2007**, *3*, 245–281.

32 Kuo, J. S.; Spicar-Mihalic, P.; Rodriguez, I.; Chiu, D. T. Electrowetting-induced droplet movement in an immiscible medium. *Langmuir* **2003**, *19*, 250–255.

33 Niu, X.; Gulati, S.; Edel, J. B.; deMello, A. J. Pillar-induced droplet merging in microfluidic circuits. *Lab Chip* **2008**, *8*, 1837–1841.

34 Bremond, N.; Thiam, A. R.; Bibette, J. Decompressing emulsion droplets favors coalescence. *Phys. Rev. Lett.* **2008**, *100*, 024501.

35 Tang, J.; Jofre, A. M.; Lowman, G. M.; Kishore, R. B.; Reiner, J. E.; Helmerson, K.; Goldner, L. S.; Greene, M. E. Green fluorescent protein in inertially injected aqueous nanodroplets. *Langmuir* **2008**, *24*, 4975–4978.

36 Jeffries, G. D. M.; Kuo, J. S.; Chiu, D. T. Controlled shrinkage and re-expansion of a single aqueous droplet inside an optical vortex trap. *J. Phys. Chem. B* **2007**, *111*, 2806–2812.

37 He, M. Y.; Sun, C. H.; Chiu, D. T. Concentrating solutes and nanoparticles within individual aqueous microdroplets. *Anal. Chem.* **2004**, *76*, 1222–1227.

38 Sgro, A. E.; Allen, P. B.; Chiu, D. T. Thermoelectric manipulation of aqueous droplets in microfluidic devices. *Anal. Chem.* **2007**, *79*, 4845–4851.

39 He, M. Y.; Edgar, J. S.; Jeffries, G. D. M.; Lorenz, R. M.; Shelby, J. P.; Chiu, D. T. Selective encapsulation of single cells and subcellular organelles into picoliter- and femtoliter-volume droplets. *Anal. Chem.* **2005**, *77*, 1539–1544.

40 Sims, C. E.; Meredith, G. D.; Krasieva, T. B.; Berns, M. W.; Tromberg, B. J.; Allbritton, N. L. Laser−micropipet combination for single cell analysis. *Anal. Chem.* **1998**, *70*, 4570–4577.

41 Kuyper, C. L.; Fujimoto, B. S.; Zhao, Y.; Schiro, P. G.; Chiu, D. T. Accurate sizing of nanoparticles using confocal correlation spectroscopy. *J. Phys. Chem. B* **2006**, *110*, 24433–24441.

42 Kuyper, C. L.; Budzinski, K. L.; Lorenz, R. M.; Chiu, D. T. Real-time sizing of nanoparticles in microfluidic channels using confocal correlation spectroscopy. *J. Am. Chem. Soc.* **2006**, *128*, 730–731.

43 Gadd, J. C.; Kuyper, C. L.; Fujimoto, B. S.; Allen, R. W.; Chiu, D. T. Sizing subcellular organelles and nanoparticles confined within aqueous droplets. *Anal. Chem.* **2008**, *80*, 3450–3457.

44 Roman, G. T.; Wang, M.; Shultz, K. N.; Jennings, C.; Kennedy, R. T. Sampling and electrophoretic analysis of segmented flow streams using virtual walls in a microfluidic device. *Anal. Chem.* **2008**, *80*, 8231–8238.

45 Hatakeyama, T.; Chen, D. L. L.; Ismagilov, R. F. Microgram-scale testing of reaction conditions in solution using nanoliter plugs in microfluidics with detection by MALDI-MS. *J. Am. Chem. Soc.* **2006**, *128*, 2518–2519.

46 Schiro, P. G.; Kuyper, C. L.; Chiu, D. T. Continuous-flow single-molecule CE with high detection efficiency. *Electrophoresis* **2007**, *28*, 2430–2438.

47 Foquet, M.; Korlach, J.; Zipfel, W. R.; Webb, W. W.; Craighead, H. G. Focal volume confinement by submicrometer-sized fluidic channels. *Anal. Chem.* **2004**, *76*, 1618–1626.